Lab on a Chip

Accepted Manuscript

RSC Publishing

www.rsc.org/loc

Registered Charity Number 207890

Microfluidic reactors for photocatalytic water purification

Ning Wang, Xuming Zhang, Yu Wang, Weixing Yu, Helen L. W. Chan

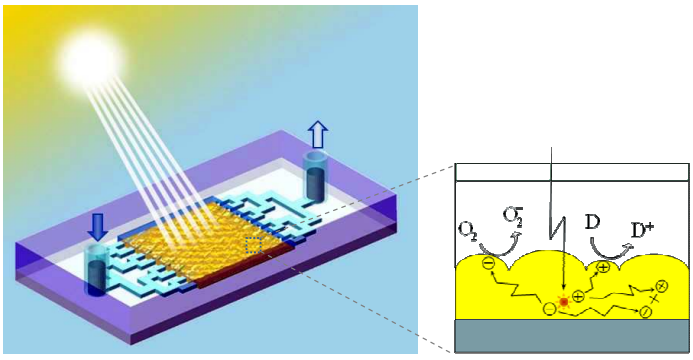

Recent studies utilize microfluidics to solve the fundamental problems of photocatalysis. Here the mechanisms and reactor designs are reviewed comprehensively.

Microfluidic reactors for photocatalytic water purification

[1,2] Ning Wang, [1, 2] Xuming Zhang*, [2]Yu Wang, [3]Weixing Yu, [2]Helen L. W. Chan

[1]*The Hong Kong Polytechnic University Shenzhen Research Institute, Shenzhen, P. R. China*

[2]*Department of Applied Physics, The Hong Kong Polytechnic University, Hong Kong S.A.R.*

[3]*State Key Laboratory of Applied Optics, Changchun Institute of Optics, Fine Mechanics and Physics, Chinese Academy of Sciences, Chang Chun, P. R. China*

E-mail: apzhang@polyu.edu.hk; Fax: 852 23337629; Tel: 852 34003258

Abstract

Photocatalytic water purification utilizes light to degrade the contaminants in water and may enjoy many merits of the microfluidics technology such as fine flow control, large surface-area-to-volume ratio and self-refreshing of reaction surface. Although a number of microfluidic reactors have been reported for photocatalysis, it is still lack of a comprehensive review. This article aims to identify the physical mechanisms that underpin the synergy of microfluidics and photocatalysis, and based on which, to review the reported microfluidic photocatalytic reactors. These microreactors help overcome different problems in the bulk reactors such as photon transfer limitation, mass transfer limitation, oxygen deficiency, and lack of reaction pathway control. They may be scaled up for large-throughput industrial applications of water process and may also find niche applications in rapid screening and standardized tests of photocatalysts.

1 Introduction

Water purification is of paramount importance to modern society due to the increasing demand of clean water and the deteriorating water supply as a result of pollution and climate change. Reclamation and reuse of wastewater could immediately increase the water resource. However, many dissolved toxic chemicals (such as dyes, pesticides, detergents) in the wastewater cannot be treated efficiently by the prevailing physical, chemical and biological water treatment methods [1-3]. As a result, the already-treated wastewater still contains some residual of contaminants and is usually discharged into rivers and seas for natural decomposition, causing a huge waste of water resources and also posing threat to environment. Photocatalytic water purification stands out as a promising remedial solution since it can decompose/mineralize a wide range of organic pollutants into innocuous products (e.g., CO_2, H_2O) under the irradiation of UV or sunlight [3-6]. In recent years, a variety of photocatalytic reactors have been reported for water treatment [3, 7-11]. But the efficiency is still limited due to many technical challenges such as mass transfer limitation, photon transfer limitation, recombination of photo-excited electrons and holes, and low selectivity of photocatalysts to visible light. Microfluidics, especially its subarea – optofluidics, may provide a quick solution to these problems.

Optofluidics is an emerging field that aims to synergize optics/photonics and microfluidics to leverage the specific advantages of both disciplines [12, 13]. It has inspired the creation of many new devices for biological sensing and chemical analysis [14, 15], imaging [16-18], optical manipulation of particles [19], energy

conversion [20, 21], and photonic systems [22, 23]. Recently, some studies start to explore the optofluidic devices to capture and control the solar energy based on a fluidic process [24-32]. Among the foci of studies is the photocatalytic water purification [33-38]. In fact, photocatalytic water purification is naturally an optofluidic system since it shares the same features of optofluidics: light, fluid and their interaction [34]. In this review, "optofluidics" and "microfluidics" are used exchangeably as a microfluidic photocatalytic reactor is naturally an optofluidic reactor.

At the first glance, microfluidics and water purification seem in contradiction since the former is designed to deal with small volume of solutions while the latter requires large throughput. This mismatch can be bridged over by scaling up the microreactors. Or alternatively, using the microreactors for the application scenarios that do not need high throughput but require repetitive tests, for example, quick test of the photocatalysts, optimization of the operational conditions and rapid screening of various photocatalysts. Compared with the conventional bulk reactors that involve large reaction plates and complicated fluidic tubing, the use of microfluidics introduces immediate benefits such as small consumptions of photocatalyst materials and water samples, precision control of flow states and short test time. Moreover, the microfluidics has more profound influence on the photocatalytic reactions in the various aspects such as mass transport, photon delivery, reaction site cleaning, new functionalities, and many others (to be elaborated in session 4).

The following parts will start with a brief introduction to the mechanism of

photocatalysis, followed by an explanation of the major problems of current photocatalytic reactors. Then benefits of microfluidics to photocatalysis will be elucidated. Next, representative designs of microfluidic reactors will be discussed in details, with the emphasis on how they help solve the existing problems of photocatalysis. Finally, niche applications of microfluidic reactors and further research will be projected.

2 Basic mechanisms of photocatalysis

Photocatalysis can be regarded as a series of oxidation and reduction reactions induced by photo-excited electrons and holes [4, 39, 40]. The mechanism is shown in Fig.1. Generally, the incoming photon with the energy $h\nu \geq E_0$ is absorbed by semiconductor photocatalysts (SC, e.g., TiO_2, ZnO) to excite an electron to the conduction band, leaving a hole in the valence band. And the activation equation can be expressed by

$$SC + h\nu \rightarrow SC(e^-_{cb} + h^+_{vb}) \quad (1)$$

Here E_0 is the bandgap of the semiconductor photocatalyst, e.g., E_0 = 3.2 eV for anatase TiO_2, corresponding to the wavelength λ = 387 nm.

The excited holes can migrate to the surface of SC and then oxidize the adsorbed reactants via the reactions as expressed below [41],

$$h^+_{vb} + {}^-OH_{ads} \rightarrow {}^\bullet OH_{ads} \quad (2)$$

$${}^\bullet OH_{ads} + \text{reactant} \rightarrow \text{Oxidized products} \quad (3)$$

This represents the hole-driven oxidation pathway.

Similarly, the excited electrons can migrate to the surface of SC too and thus can initiate a reduction reaction (e.g., $Hg^{2+} + 2e^- \rightarrow Hg^0$). Alternatively, the electrons can be captured by dissolved O_2 molecules and can also contribute to the oxidation through different pathways [41],

$$e_{cb}^- + O_{2,ads} \rightarrow O_2^{\bullet -} \quad (4)$$

$$O_2^{\bullet -} + H^+ \rightarrow HO_2^{\bullet} \quad (5)$$

$$HO_2^{\bullet} + HO_2^{\bullet} \rightarrow H_2O_2 + O_2 \quad (6)$$

$$H_2O_2 + e_{cb}^- \rightarrow {}^{\bullet}OH + OH^- \quad (7)$$

$$\text{reactant} + O_2^{\bullet -} \text{ (or } {}^{\bullet}OH) \rightarrow \text{degradation products} \quad (8)$$

These form the electron-driven oxidation pathway. It is noted that the production of hydrogen peroxide (Eq. (6)) provides much more hydroxyl radicals (Eq. (7)), which have super oxidativity in aqueous. Although both electrons and holes can lead to oxidation, some research studies have found that the electron-driven oxidation is apparently more efficient in degrading some organic contaminants (e.g., methylene blue dye).

3 Major limitations of current photocatalytic reactors

Currently, photocatalytic water purification is facing several major limitations, such as *low mass transfer efficiency*, *low photon transfer efficiency* and *deficiency of dissolved oxygen* [4, 36]. The mass transfer efficiency affects how easy the contaminant particles are moved to the photocatalyst surface (mostly determined by the surface area per unit volume, namely, SA:V) and how fast the redox products are removed

(affected by the desorption, diffusion and stirring). The photon transfer refers to how to deliver the photons to the photocatalyst reaction sites, a uniform irradiation is often required for better utilization of the photons [4, 7, 42]. For the dissolved oxygen, the electron-driven oxidation consumes oxygen, and thus the limited concentration of naturally dissolved oxygen in water (typically 10 mg/l at room temperature and 1 atmosphere) would affect the photodegradation.

Undoubtedly, reactor designs play a crucial role in tackling these limiting factors of photocatalysis and have attracted numerous efforts in the last thirty years [7, 8], leading to a number of innovative reactor designs such as packed bed photoreactors [9], fluidized bed reactors [10, 11], thin film bed sloping plate reactors [3], and many others. Most are referred as bulk reactors due to the large dimension of the reactor systems. Generally, the bulk reactors can be classified into two main types, depending on the formations of photocatalysts: (1) *slurry reactor*, in which the photocatalyst nanoparticles are suspended in water samples to form a slurry (see Fig. 1 (b)); and (2) *immobilized reactor*, in which the photocatalyst is immobilized on the substrates in the form of film coating (see Fig. 1 (b)). The former has large SA:V and enjoys fast mass transfer, but the absorption and scattering by the suspended photocatalyst nanoparticles cause a non-uniform distribution of light and thus low photon transfer. In addition, the suspended nanoparticles need to be filtered out after the purification, increasing the operation difficulty. In contrast, the latter type has good photon transfer and no need for post-filtration, but the low SA:V causes a slow mass transfer.

Various reactors have been attempted to break these limitations. For example,

spin disc reactors [43] were designed to overcome the mass transfer limitation, optical fiber based reactors [44-46] were used to tackle the photon transfer limitation, and some reactors injected H_2O_2 or O_2 to solve the oxygen deficiency [47-48]. However, most of them aim at either one aspect or two, but none could get rid of all the limitations.

4 Benefits of microfluidics to photocatalysis

Microfluidics technology employs microstructures to handle small volume of fluids and exhibits remarkable capabilities in fine flow control, wide tunability and parallel analysis [49-51]. Its great success in bioanalysis and drug discovery has triggered a boom of research to apply microfluidics to other areas, one of which is the photocatalysis.

The microfluidics could bring in many benefits to the photocatalysis. The prominent ones are described below.

(1) Large surface area: Microfluidic structures have inherently large SA:V due to the small volume of fluid [33-36, 42, 48, 52-75], typically in the range of 10,000 – 300,000 m^2/m^3, at least two orders of magnitude larger than the bulk reactors (typically < 600 m^2/m^3) [7, 8, 40, 46]. For this reason, significant enhancement of the reaction rate has been observed in the microfluidic reactors (called *microreactors* hereafter) as compared to the bulk reactors. It is noted that SA:V here refers to the nominal surface area of the water sample over the water volume. For a microreactor with a rectangular bottom and a height h, it has SA:V = $1/h$. In an real microreactor,

SA:V could be much larger if the photocatalyst film is nanoporous.

(2) Short diffusion length: The microfluidic layer is typically very thin (10 – 100 μm), making it easy for the organic pollutants to diffuse to the reaction surface.

(3) Uniform residence time: The flow in microfluidic structures is typically laminar. This is not ideal for diffusion, but it ensures almost the same residence time (i.e., the time for the water sample to flow through the reactor, equivalent to the photocatalytic reaction time) and thus an equal level of degradation for different parts of the microflows. As the reaction rate (i.e., the percentage of pollutants converted per unit time) decreases with longer residence time [34], an even distribution of residence time helps maximize the throughput (the processed water volume per unit time) at a targeted degradation percentage (i.e., how much percent being degraded [41]).

(4) Uniform illustration: The microreactors usually have an immobilized photocatalyst film under the thin layer of fluid, resulting in an almost uniform irradiation over the whole reaction surface and thus a high photon efficiency. This is because the reaction rate constant of semiconducting photocatalysts is usually proportional to the square root of power density [4].

(5) Short reaction time: The combination of above factors drastically improves the reaction speed and thus shortens the reaction time. In microreactors, it takes only several to tens of seconds to obtain significant degradation (e.g., 90% degraded) [34-36], whereas the bulk reactors usually needs several hours [64].

(6) Self-refreshing effect: The running fluid naturally refreshes the reaction surface, which helps move away the reaction productions and increases the stability of the

photocatalysts. In the bulk reactors, typically the activity of photocatalysts degrades noticeably after 10 runs of photocatalytic reactions [7, 8, 40, 46], whereas in the microreactors the photocatalysts can easily last for several hundred runs of reactions [36].

(7) Optimization of operation condition: The fine control of fluids enables to optimize the operation condition of photocatalysis. For instance, by slowing down the flow rate and/or disturbing the laminar flows, the microreactors could clean most of the contaminants in one run, without resorting to the recirculation of flows, which is a common practice in the bulk reactors [7, 8, 40, 46].

(8) More functionalities: The microfluidics has the potential to add more functionalities to the photocatalysis, such as fast heat transfer, parallel process for rapid screening of photocatalysts, micro-mixing [33], on-chip monitoring of photocatalytic reactions, controllable delivery of light using optofluidic waveguides [24-32], selection of reaction pathways [36], and so on.

5 Review of microreactors for photocatalytic water purification

Various microreactors have been explored for photocatalytic reactions such as water purification, water splitting [37, 38], photosynthesis [66-75], bioparticle deactivation and heavy metal ion mineralization. Here we limit the survey to only the water purification because it is simplest and most representative. A brief survey of the reported microreactors for photocatalytic studies is listed in Table 1. Although their designs vary significantly, they can be simply classified into four configurations as

schemed in Fig. 2. The major difference can be seen more clearly from the transverse cross section (perpendicular to the flow direction) of the reactors. The *micro-capillary reactor* coats a layer of photocatalyst on the inner wall of a capillary tube and runs the water sample inside the tube. The light can be irradiated from the outside. The *single-microchannel reactor* makes use a single straight microchannel to carry the water sample whereas the *multi-microchannel reactor* exploits an array of the microchannels. The *planar microreactor* enlarges the microchannel in the lateral direction into a planar chamber. The first three configurations are based on microchannels, each of which has comparable dimensions of width and height (or diameter) in the range of 10 – 100 μm, whereas the last one has a much larger width (typically 1 – 100 mm) than the height. For photocatalysis, such a difference significantly affects the throughput, the photon utilization, the fabrication of photocatalysts, and the scalability to macro-scale reactors.

5.1 Micro-capillary reactors

An early work was reported by Li *et al*. [76], who fabricated a microreactor using capillaries with an inner diameter of 200 μm (see Fig. 3 (a)). The inner wall was coated with TiO_2/SiO_2 film to degrade the aqueous methylene blue (MB) solution. Micro-capillary based reactors have also been used to decompose various other organic dyes [77-79]. It is the simplest design, but the coating on the inner wall is cumbersome. And the external irradiation is not ideal for the utilization of light because the outer part of the photocatalyst layer absorbs light but makes little

contribution to the photodegradation.

5.2 Single-microchannel reactors

With rapid development of various etching techniques such as photolithography, micro/nano imprinting and dry/wet etching, some researchers fabricated microchannels on glass, ceramic and polymer substrates to examine photocatalytic reactions. Matsushita *et al.* designed a single straight microchannel to degrade some organic models [80] (see Fig. 3 (b)). The bottom of microchannel was immobilized with a sol-gel prepared TiO_2 thin film loaded with Pt particles. Similar reactors using single straight microchannels can be found in many other studies on the degradation of organic contaminants [80-83].

5.3 Multi-microchannel reactors

The microreactors based on micro-capillary and single microchannel have small photon receiving areas and waste most of the external irradiation light. And the small cross-sectional area limits the throughput as well. To tackle these problems, multiple microchannels have been introduced. In 2004, Gorges *et al*. [54] designed a microreactor that branched out 19 parallel microchannels. It immobilized a TiO_2 nanoporous film and fixed a UV-LED array above the area of the branched microchannels. The illuminated specific surface of the microreactor surpassed that of conventional bulk reactors by two orders of magnitude. In 2005, Takei *et al.* [52] fabricated a multi-microchannel reactor for photocatalytic redox-combined synthesis

of L-pipecolinic acid using an anatase TiO_2 thin film (see Fig. 3 (c)). Pt nanoparticles were photodeposited from H_2PtCl_6 as the reduction site. It found that the conversion rate in the microreactor was 70 times larger than that in a cuvette using titania nanoparticles with almost the same selectivity and enantiomeric excess. In another form of the multi-microchannel reactor, a single microchannel is folded up into a serpentine shape (see Fig. 3 (d)) [33, 48, 84]. This increases the photon receiving area and the residence time. However, the cross section remains the same as that of a single microchannel and thus limits the throughput.

5.4 Planar microreactors

To further enhance the utilization of the surface area of microfluidic chips, planar microreactors have been proposed. We fabricated the microreactor of this type to study the photocatalytic degradation of MB under solar irradiation [34]. The design and cross-section of microreactor can be seen in Fig. 4 (a) and (b). The microreactor had a rectangular reaction chamber, which was constructed by two nanoporous TiO_2-coated glasses [72] as the cover and substrate and a 100-μm-thick epoxy layer as the spacer and sealant. The scanning electron micrographs of nanoporous film are also shown in Fig. 4 (c). In the planar microreactor, the TiO_2 films on the glasses had the same surface area with the reaction chamber, making the best use of surface area for light receiving and photocatalytic reaction. In this device, the liquid layer was 100 μm thick, and thus the nominal SA:V of the microreactor was $\mathrm{SA:V} = 2/h_2 = 20{,}000\ \mathrm{m}^{-1}$, where h_2 is the height of reaction chamber (see Fig.

4(b)). As mentioned above, the actual value should be many times larger due to the nanoporous morphology of TiO_2 film. Such a high SA:V would significantly improve the mass transfer efficiency. From the experimental results plotted in Fig. 4 (d), the photodegradation efficiency of MB could go up to 94% at a reaction time of 36 s, which was really impressive as compared to the reaction time of several hours or even days that are often needed in the bulk reactors [64]. The experimental data showed that the reaction rate constant was enhanced by > 100 times as compared to the bulk reactors. However, the device faced the problems of oxygen deficiency (due to the insufficient dissolved oxygen) and low solar spectrum sensitivity (due to the use of TiO_2). In addition, the recombination of photo-excited electrons and holes was still quite serious because of the use of one type of photocatalyst material (i.e., TiO_2) and thus no internal mechanism to separate electrons and holes.

To solve these problems, we designed another planar microreactor [36] as shown in Fig. 5. At the bottom of reaction chamber, a nanoporous layer of monoclinic $BiVO_4$ (BVO) was deposited onto an indium tin oxide (ITO) glass (see Fig. 5 (b)). BVO had high photocatalytic reactivity under visible light because of its small bad gap (< 2.7 eV) and good charge migration ability. This ensured a better utilization of the solar spectrum. The top of reaction chamber was an ITO glass too, and it was connected to the bottom ITO glass through a voltage source. When a bias voltage was applied, the electrons and holes were forced to separate. In fact, the bias voltage introduced other benefits. By changing the polarity of voltage, electrons or holes could be selectively driven to the BVO reaction surface. This enabled the control of electron-driven or

hole-driven oxidation for photodecomposition (see the insets of Fig. 5 (c)). In addition, when the top ITO layer was driven over 1.23 V, electrolysis of water generated oxygen, which could diffuse to the BVO surface to supply the oxygen for electron-driven oxidation. In this way, it solved the oxygen deficiency problem. From the experimental results in Fig. 5 (c), the negative bias exhibited always higher performance. The device was tested for more than 200 times and showed little degradation of the performance.

6 Discussions and Outlook

The microfluidic reactors have some limitations too. It involves the fabrication of microstructures and the embedment of photocatalysts. Fortunately, fabrication of microfluidic structures using soft materials (but may have hard cover and hard substrate) is already a routine process, and the photocatalyst can be deposited onto the substrate before being bonded with the microstructure. Another severe problem is the limited throughput, typically in 1 ml/h. This is far from the threshold throughput of about 1,000 l/h for practical applications. To boost up the throughput, several possible approaches could be exploited. A simple way is to use a large array of microreactors to sum up the throughput to a meaningful level (like 1 l/h). A more practical way is to scale up the microreactors to the meter size, while maintaining the performance determining factors such as surface-area-to-volume ratio and the residence time. We have already developed the reactors with the footprint of half of an A4 paper to clean water at 1 l/h and are moving toward large reactors (2 m × 2 m × 0.5 m, L×W×H) for

1000 l/h. New designs could also been introduced, for example, coating the inner surface of capillary tubes with photocatalysts and then piling up the tubes into a large bundle (similar to the structure of a photonic crystal fiber but having much cross section). This design is a combined use of optofluidic waveguide and photonic crystal fiber. The contaminated water could be run through the holes of tubes and the light may be irradiated directly onto the bundle cross section. Each stream of flow inside the tubes acts as an optofluidic waveguide to carry the light, which is absorbed gradually by the photocatalyst layer coated on the tube inner surface for photodegradation. This design ensures a long interaction length of the light with the photocatalyst layer and the water sample, and would lead to a full utilization of the light energy and a total cleaning of the contaminants. Large cross-sectional area and fast flow velocity (using long tubes to ensure sufficient residence time) join up for large throughput. It is feasible to achieve 1000 l/h. Many other innovative designs could be explored as well. With the techniques and physical understandings accumulated during the development of microfluidic reactors, the prospect for industrial water purification is very promising.

On the other hand, there are many scenarios that do not need large throughput. In fact, the microreactors consume small amounts of liquid sample and photocatalysts. This could be a beneficial factor for some applications, for instance, rapid characterization of expensive photocatalysts, parallel performance comparison of different photocatalysts and optimization of the operation condition. As the photocatalytic reaction is strongly dependent on many factors (e.g., type of

photocatalysts, preparation details of photocatalysts, model chemicals, light sources, temperature, pH value, etc.), it has long been a headache to standardize the photocatalytic efficiency tests and to make different tests comparable. The microreactors may provide a standard platform as it enables convenient control of operation conditions (such as flow rate, heat dissipation, etc), rapid characterization and parallel photoreactions (using an array of microchannels or reaction chambers). Similar case in the use of microfluidic chips for drug screening has achieved great success.

Beyond that, the microreactors have potential for other fields. Actually, some studies have already tried water splitting [37, 38], protein cleavage [65] and photosynthesis [66-75], but most are on the infant stage. There are still a lot more to explore. For example, bulk reaction systems have utilized the photocatalysis for destructing bacteria [85] and viruses [86], inactivation of cancer cells [87], nitrogen fixation [88, 89] and remediation of oil spills [47, 90]. Their corresponding microfluidic designs have yet to come.

Acknowledgement

XMZ would like to acknowledge the financial supports of National Science Foundation of China (No. 61377068), Research Grants Council (RGC) of Hong Kong (No. N_PolyU505/13) and the Hong Kong Polytechnic University (PolyU 5034/13P, 1-ZVAW, A-PL16 and A-PM21).

References

[1] M. A. Shannon, P. W. Bohn, M. Elimelech, J. G. Georgiadis, B. J. Mariňas, and A. M. Mayes, *Nature*, 2008, **452**, 301–310.

[2] P. R. Gogate and A. B. Pandit, *Adv. Environ. Research*, 2004, **8**, 501–551.

[3] D. F. Ollis and H. Al-Ekabi (eds.), *Photocatalytic Purification and Treatment of Water and Air*, Elsevier, Amsterdam, 1993.

[4] J. M. Herrmann, *Catal. Today*, 1999, **53**, 115–129.

[5] P. R. Gogate and A. B. Pandit, *AIChE J.*, 2004, **50**, 1051–1079.

[6] A. Mills, S.K. Lee, *Semiconductor Photocatalysis*, in: S. Parsons (ed.), *Advanced Oxidation Processes for Water and Wastewater Treatment*, IWA Publishing, London, 2004.

[7] T. Van Gerven, G. Mul, J. Moulijn, and A. Stankiewicz, *Chem. Engin. Process.*, 2007, **46**, 781–789.

[8] C. McCullagh, N. Skillen, M. Adams and P. K.J. Robertson, *J. Chem. Technol. Biotechnol.*, 2011, **86**, 1002–1017.

[9] M. Mehrvar, W. A. Anderson and M. Moo-Young, *Adv. Environ. Res.*, 2002, **6**, 411–418.

[10] H. P. Kuo, C. T. Wu and R. C. Hsu, *Powder Technol*., 2009, **195**, 50–56.

[11] D. K. Lee, S. C. Kim, I. C. Cho, S. J. Kim and S. W. Kim, *Sep. Purif. Technol.*, 2004, **34**, 59–66.

[12] D. Psaltis, S.R. Quake and C. Yang, *Nature*, 2006, **442**, 381–386.

[13] Y. Fainman, D. Psaltis, L. Lee and C. Yang, *Optofluidics: Fundamentals, Devices and Applications*, McGraw-Hill, 2009.

[14] F. B. Myers and L. P. Lee, *Lab Chip*, 2008, **8**, 2015–2033.

[15] X. D. Fan and I. M. White, *Nat. Photon.*, 2011, **5**, 591–597.

[16] X. Heng, D. Erickson, L. R. Baugh, Z. Yaqoob, P. W. Sternberg, D. Psaltis, and C. H. Yang, *Lab Chip*, 2006, **6**, 1274–1276.

[17] X. Q. Cui, L. M. Lee, X. Heng, W. W. Zhong, P. W. Sternberg, D. Psaltis, and C. H. Yang, *Proc. Natl. Acad. Sci.*, 2008, **105**, 10670–10675.

[18] O. Mudanyali, D. Tseng, C. Oh, S. O. Isikman, I. Sencan, W. Bishara, C. Oztoprak, S. Seo, B. Khademhosseinia, and A. Ozcan, *Lab Chip*, 2010, **10**, 1417–1428.

[19] P. Y. Chiou, A. T. Ohta, and M. C. Wu, *Nature*, 2005, **436**, 370–372.

[20] D. Erickson, D. Sinton, and D. Psaltis, *Nat. Photon.*, 2011, **5**, 583–590.

[21] Y. F. Chen, L. Jiang, M. Mancuso, A. Jain, V. Oncescu, and D. Erickson, *Nanoscale*, 2012, **4**, 4839–4857.

[22] C. Monat, P. Domachuk and B. J. Eggleton, *Nat. Photon.*, 2007, **1**, 106–114.

[23] H. Schmidt and A. R. Hawkins, *Nat. Photon.*, 2011, **5**, 598–604.

[24] K. Mori, *Biotechnol. Bioeng. Symp.*, 1985, **15**, 331–345.

[25] K. Mori, H. Ohya, K. Matsumoto, H. Furuune, K. Isozaki and P. Siekmeier, *Adv. Space Res.*, 1989, **9**, 161–168.

[26] S. A. Angermayr, K. J. Hellingwerf, P. Lindblad and M. J. de Mattos, *Curr. Opin. Biotech.*, 2009, **20**, 257–263.

[27] F. Lehr and C. Posten, *Curr. Opin. Biotech.*, 2009, **20**, 280–285.

[28] T. V. Laurinavichene, A. S. Fedorov, M. L. Ghirardi, M. Seibert, and A. A. Tsygankov, *Int. J. Hydrog. Energy*, 2006, **31**, 659–667.

[29] D. J. Bayless, G. Kremer, M. Vis, B. Stuart, L. Shi, E. Ono and J.L. Cuello, *J. Env. Eng. Manag.*, 2006, **16**, 209–215.

[30] S. Atsumi, W. Higashide and J. C. Liao, *Nat. Biotechnol.*, 2009, **27**, 1177–1180.

[31] C. Tan, S-J Lo, P. R. LeDuc and C-M Cheng, *Lab Chip*, 2012, **12**, 3654–3665.

[32] E. E. Coyle and M. Oelgemöller, *Photochem. Photobiol. Sci.*, 2008, **7**, 1313–1322.

[33] Z. X. Meng, X. Zhang and J. H. Qin, *Nanoscale*, 2013, **5**, 4687–4690.

[34] L. Lei, N. Wang, X. M. Zhang, Q. D. Tai, D. P. Tsai and Helen L.W. Chan, *Biomicrofluid.*, 2010, **4**, 043004.

[35] N. Wang, Z. K. Liu, N. Y. Chan, H. L. W. Chan and X. M. Zhang, MicroTAS 2012, Okinawa, Japan, paper W.9.195.

[36] N. Wang, X. M. Zhang, B. L. Chen, W. Z. Song, N. Y. Chan, and H. L. W. Chan, *Lab Chip*, 2012, **12**, 3983–3990.

[37] S. S. Ahsan, A. Gumus, and D. Erickson, *Lab Chip*, 2013, **13**, 409–414.

[38] Y. Matsushita, H. Mohamed, A. Mohamed, and S. Ookawara, μTAS 2012, Okinawa, Japan.

[39] X. M. Zhang, Y. L. Chen, R-S Liu and D. P. Tsai, *Rep. Prog. Phys.* 2013, **76**, 046401.

[40] Y. L. Chen, L-C Kuo, M. L. Tseng, H. M. Chen, C-K Chen, H. J. Huang, R-S Liu, and D. P. Tsai, *Opt. Express*, 2013, **21**, 7240–7249.

[41] J. M. Herrmann, *J. Photochem. Photobiol. A*, 2010, **216**, 85–93.

[42] H. Lu, M. A. Schmidt, and K. F. Jensen, *Lab Chip*, 2001, **1**, 22–28.

[43] T. V. Nguyen and J. C. S. Wu, *Sol. Energy Mat. Sol. Cells*, 2008, **92**, 864–872.

[44] C. N. Lin, C. Y. Chang, H. J. Huang, D. P. Tsai, and N. L. Wu, *Environ. Sci. Pollut. Res.*, 2012, **19**, 3743–3750.

[45] N. J. Peill and M. R. Hoffmann, *Environ. Sci. Technol.*, 1995, **29**, 2974–2980.

[46] J. C. S. Wu, T-H Wu, T. Chu, H. Huang, and D. P. Tsai, *Top Catal.*, 2008, **47**, 131–136.

[47] E. Bessa, G. L. Sant'Anna and M. Dezotti, *Appl. Catal. B-Environ.*, 2001, **29**,

125–134.

[48] H. Lindstrom, R. Wootton, and A. Iles, *AIChE J.*, 2007, **53**, 695–702.

[49] T. M. Squires and S. Quake, *Rev. Mod. Phys.*, 2005, **77**, 977–1026.

[50] G. M. Whitesides, *Nature*, 2006, **442**, 368–373.

[51] N-T Nguyen and S. T. Wereley, *Fundamentals and Applications of Microfluidics (2nd ed.)*, Artech House, Boston, 2006.

[52] G. Takei, T. Kitamori, and H. B. Kim, *Catal. Commun.*, 2005, **6**, 357–360.

[53] R. C. R. Wootton, R. Fortt, and A. J. de Mello, *Org. Process Res. Dev.*, 2002, **6**, 187–189.

[54] R. Gorges, S. Meyer, and G. Kreisel, *J. Photochem. Photobiol. A*, 2004, **167**, 95–97.

[55] M. Mohseni, *Chemosphere*, 2005, **59**, 335–342.

[56] G. Vincent, P. M. Marquaire and O. Zahraa, *J. Photochem. Photobiol. A*, 2008, **197**, 177–189.

[57] P. K. Dutta and A. K. Ray, *Chem. Eng. Sci.*, 2004, **59**, 5249–5259.

[58] J. G. Sczechowski, C. A. Koval and R. D. Noble, *Chem. Eng. Sci.*, 1995, **50**, 3163–3173.

[59] R. C. Giordano, R. L. C. Giordano, D. M. F. Prazeres, and C. L. Cooney, *Chem. Eng. Sci.*, 1998, **53**, 3635–3652.

[60] O. Richter, H. Hoffmann and B. Kraushaar-Czarnetzki, *Chem. Eng. Sci.*, 2008, **63**, 3504–3513.

[61] G. Li Puma and P. L. Yue, *Environ. Sci. Technol.*, 1999, **33**, 3210–3216.

[62] E. Sahle-Demessie, S. Bekele and U. R. Pillai, *Catal. Today*, 2003, **88**, 61–72.

[63] Z. Zhang, W. A. Anderson and M. Moo-Young, *Chem. Eng. J.*, 2004, **99**, 145–152.

[64] M. Oelgemöller, *Chem. Eng. Technol.*, 2012, 35, 1144–1152.

[65] B. Jones, L. Locascio and M. Hayes, MicroTAS, 2005, Boston.

[66] J. R. Adleman, D. A. Boyd, D. G. Goodwin, and D. Psaltis, *Nano Lett.*, 2009, **9**, 4417–4423.

[67] J. S. Lee, S.H. Lee, J.H. Kim, and C.B. Park, *Lab Chip*, 2011, **11**, 2309–2311.

[68] Y. Matsushita, T. Ichimura, N. Ohba, S. Kumada, K. Sakeda, T. Suzuki, H. Tanibata, and T. Murata, *Pure Appl. Chem.*, 2007, **79**, 1959–1968.

[69] Y. Matsushita, N. Ohba, S. Kumada, T. Suzuki, and T. Ichimura, *Catal. Commun.*, 2007, **8**, 2194–2197.

[70] Y. Matsushita, N. Ohba, T. Suzuki, and T. Ichimura, *Catal. Today*, 2008, **132**, 153–158.

[71] Y. Matsushita, S. Kumada, K. Wakabayashi, K. Sakeda, and T. Ichimura, *Chem. Lett.*, 2006, **35**, 410–411.

[72] N. Wang, L. Lei, X. M. Zhang, Y. H. Tsang, Y. Chen, and H. L.W. Chan, *Microelectron. Engin.*, 2011, **88**, 2797–2799.

[73] M. Neumann and K. Zeitler, *Org. Lett.*, 2012, **14**, 2658–2661.

[74] N. B. Jackson, C. M. Wang, Z. Luo, J. Schwitzgebel, J. G. Ekerdt, J. R. Brock, and A. Heller, *J. Electrochem. Soc.*, 1991, **138**, 3660–3664.

[75] P. C. K. Vesborg, S. In, J. L. Olsen, T. R. Henriksen, B. L. Abrams, Y. Hou, A. Kleiman-shwarsctein, O. Hansen, and I. Chorkendorff, *J. Phys. Chem. C*, **114**, 11162 (2010).

[76] X. Li, H. Wang, K. Inoue, M. Uehara, H. Nakamura, M. Miyazaki, E. Abea, and H. Maeda, *Chem. Commun.*, 2003, **8**, 964–965.

[77] K. Oda, Y. Ishizaka, T. Sato, T. Eitoku, and K. Katayama, *Analyt. Sci.*, 2010, **26**, 969–972.

[78] Z. Zhang, H. Wu, Y. Yuan, Y. Fang, and L. Jin, *Chem. Engin. J.*, 2012, **184**, 9–15.

[79] N. Tsuchiya, K. Kuwabara, A. Hidaka, K. Oda, and K. Katayama, *Phys. Chem. Chem. Phys.*, 2012, **14**, 4734–4741.

[80] Y. Matsushita, N. Ohba, S. Kumada, K. Sakeda, T. Suzuki, and T. Ichimura, *Chem. Engin. J.*, 2008, **135**, S303–S308.

[81] G. Charles, T. Roques-Carmes, N. Becheikh, L. Falk, J.-M. Commenge, and S. Corbel, *J. Photochem. Photob. A*, 2011, **223**, 202–211.

[82] D. Daniel and I. G. R. Gutz, *Electrochem. Commun.*, 2007, **9**, 522–528.

[83] T. H. Yoon, L.-Y. Hong, and D.-P. Kim, *Chem. Engin. J.*, 2011, **167**, 666–670.

[84] H. C. Aran, D. Salamon, T. Rijnaarts, G. Mul, M. Wessling, and R. G. H. Lammertink, *J. Photochem. Photobiol. A*, 2011, **225**, 36–41.

[85] J. C. Ireland, P. Klostermann, E. W. Rice, and R. M. Clark, *Appl. Environ. Microbiol.*, 1993, **59**, 1668–1670.

[86] J. C. Sjogren and R. A. Sierka, *Appl. Envrion. Microbiol.*, 1994, **60**, 344–347.

[87] R. Cai, K. Hashimoto, Y. Kubota and A. Fujishima, *Chem. Lett.*, 1992, **3**, 427–430.

[88] M. Schiavello, *Electrochim Acta*, 1993, **38**, 11–14.

[89] M. M. Taqui Khan, D. Chatterjee and M. Bala, *J. Photochem. Photobiol. A*, 1992, **67**, 349–352.

[90] H. Gerischer and A. Heller, *J. Electrochem. Soc.*, 1992, **139**, 113–118.

List of table titles

Table 1 Typical microfluidic reactors used for photocatalytic water treatment.

List of figure captions

Fig. 1 (a) Basic principle of photocatalysis. The semiconductor photocatalytic nanoparticle absorbs a photon and excites an electron/hole pair. The electron and hole then migrate to the surface and initiate the reduction and/or oxidation to decompose the water contaminants. (b) Typical bulk reactor designs – slurry reactor and immobilized reactor.

Fig. 2 Typical designs of microfluidic reactors for photocatalysis water purification. (a) Transverse cross-section of micro-capillary reactor; (b) single-microchannel reactor; (c) multi-microchannel reactor; and (d) planar microreactor.

Fig. 3 Demonstrated microchannel-based reactors. (a) Micro-capillary reactor with the inner wall coated with self-assemble SiO_2/TiO_2 for methylene blue degradation, the dimensions of capillary: 5 cm (length) × 530 μm (outer diameter) and 200 μm (inner diameter) [76]; (b) single straight microchannel reactor with immobilized TiO_2-coated silica beads for degradation of 4-chlrophenol [80]; (c) branched microchannel reactor for synthesis of L-pipecolinic acid [52]; (d) serpentine microchannel reactor having 11 rows with 32 side lobes per row, coated with porous TiO_2 on the inner wall, for methylene blue degradation [48].

Fig. 4 Planar microreactor using immobilized nanoporous TiO_2 film for methylene blue decomposition [34]. (a) Schematic diagram and (b) cross-section of the microreactor; (c) scanning electron micrographs of the nanoporous TiO_2 film; (d) characterization of photocatalytic performance of microreactor.

Fig. 5 Photoelectrocatalytic (PEC) microreactor based on the planar configuration [36]. (a) Photo of the PEC microreactor; (b) working principle of PEC under the negative bias larger than water electrolysis potential. The electrolyzed oxygen on the anode can migrate to the photocatalyst surface to supply oxygen for photocatalytic oxidation; (c) measured performances in degrading methylene blue under different bias potentials. The results under negative bias are shown in the left panel and those under positive bias are in the right panel.

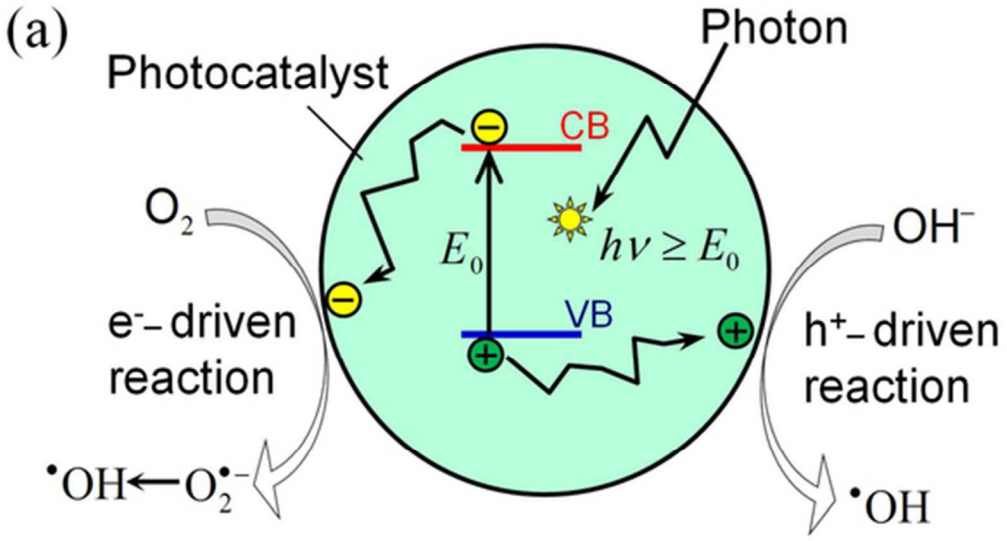

49x26mm (300 x 300 DPI)

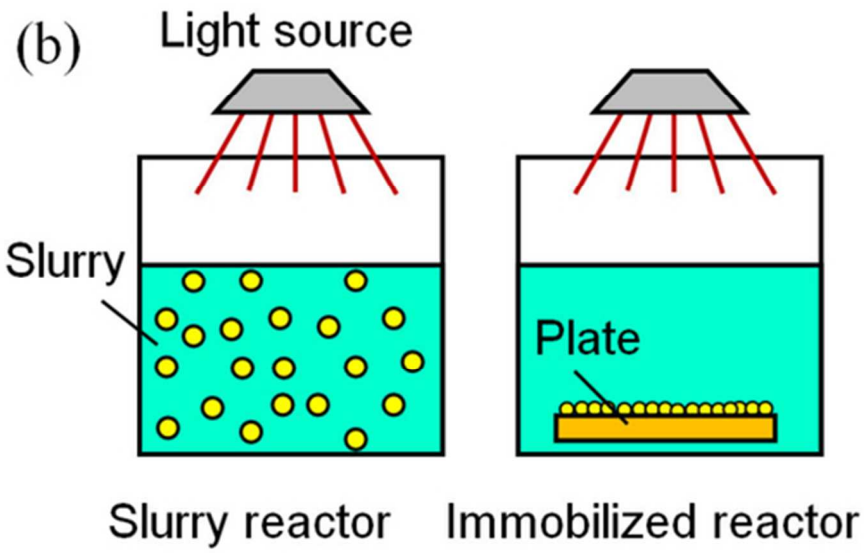

49x26mm (300 x 300 DPI)

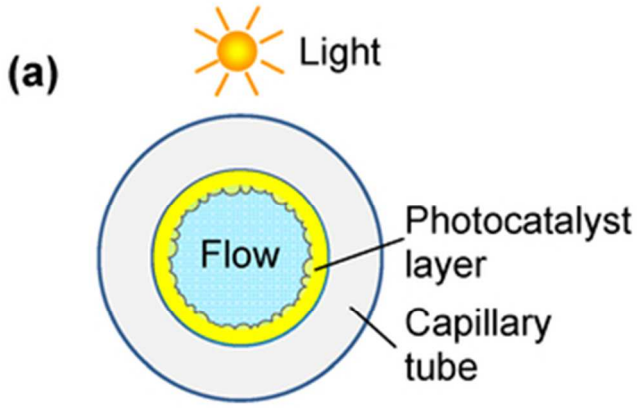

35x17mm (300 x 300 DPI)

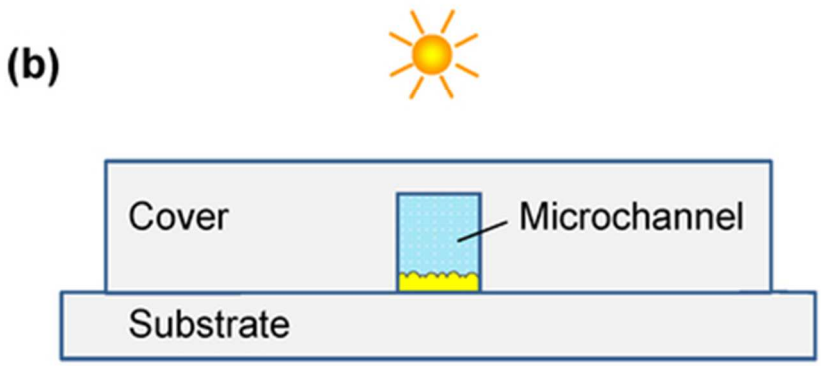

35x17mm (300 x 300 DPI)

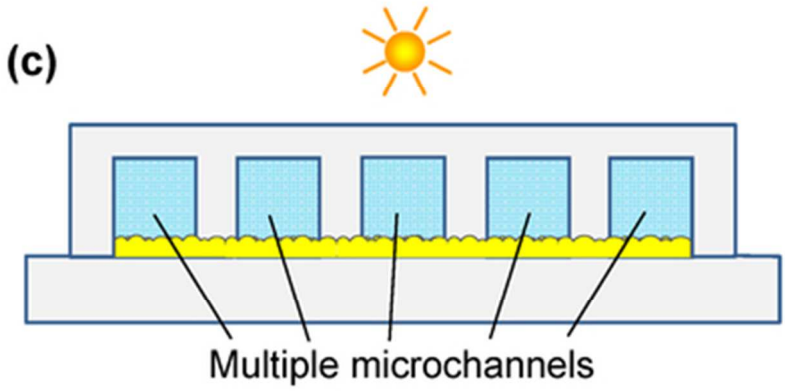

35x17mm (300 x 300 DPI)

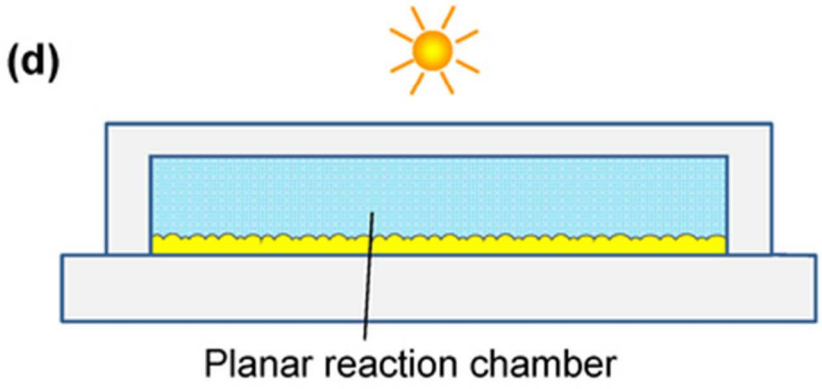

35x17mm (300 x 300 DPI)

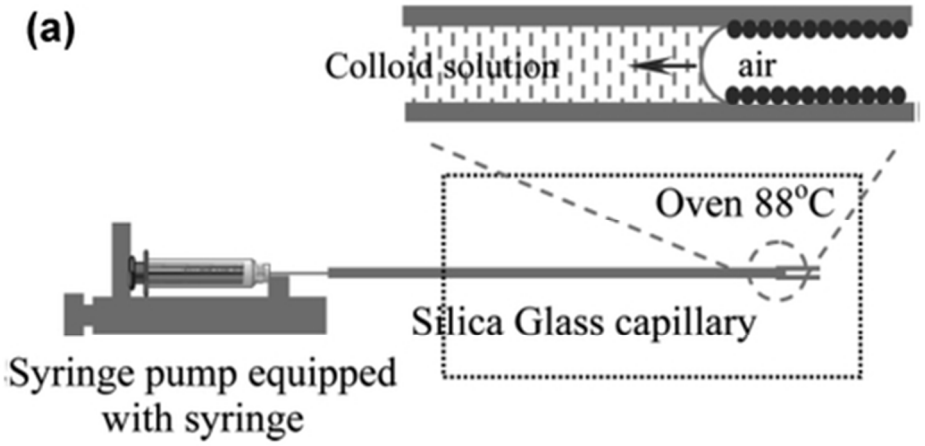

39x19mm (300 x 300 DPI)

(b)

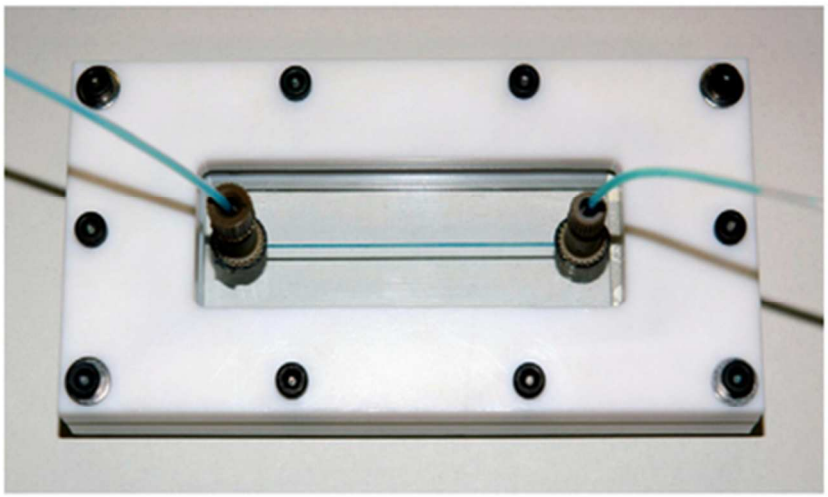

39x22mm (300 x 300 DPI)

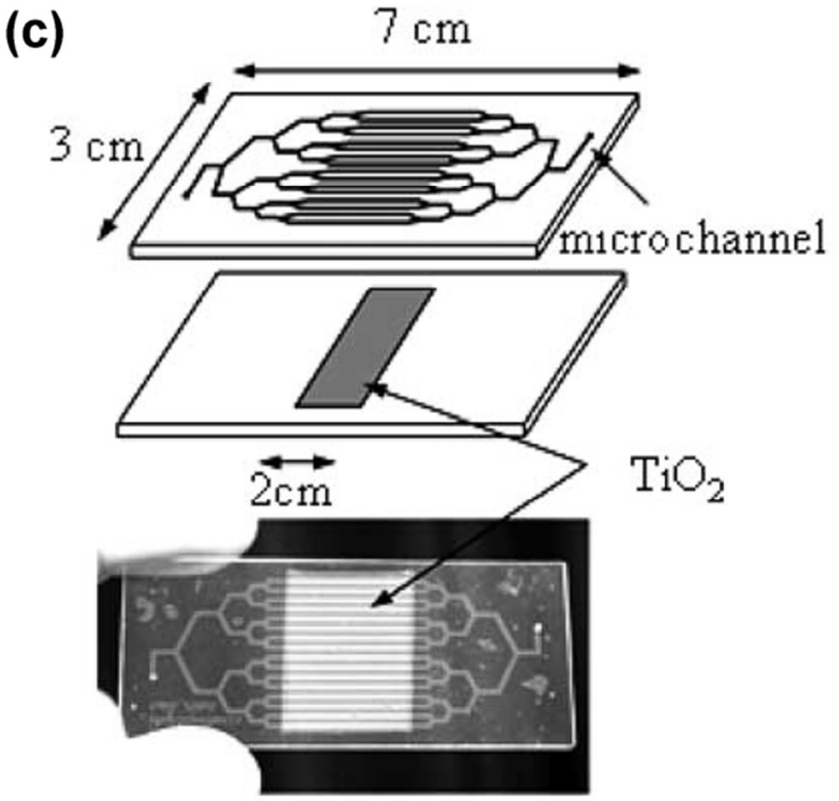

58x49mm (300 x 300 DPI)

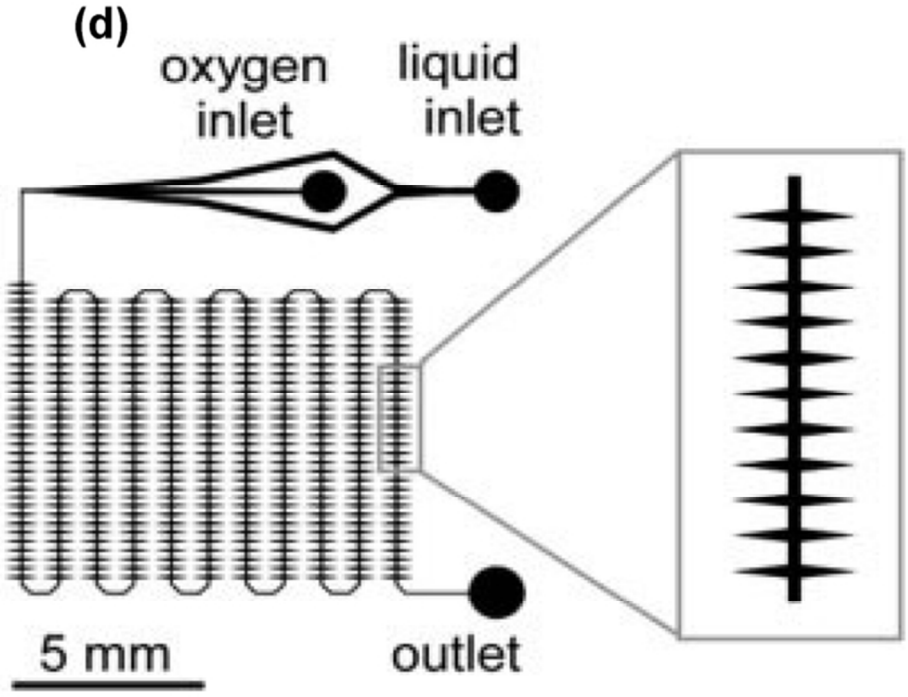

58x42mm (300 x 300 DPI)

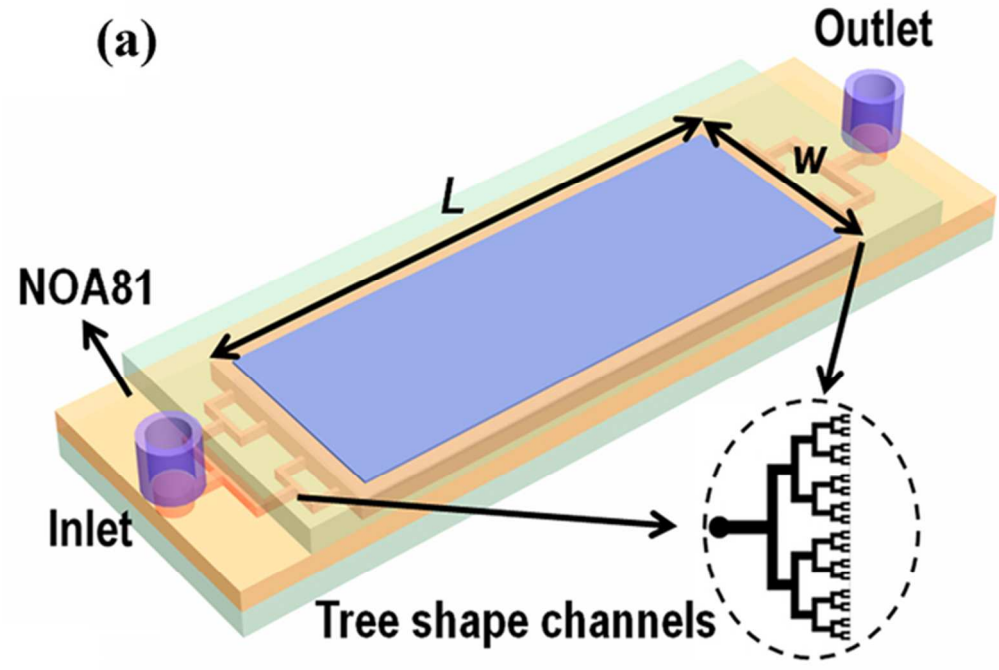

53x36mm (300 x 300 DPI)

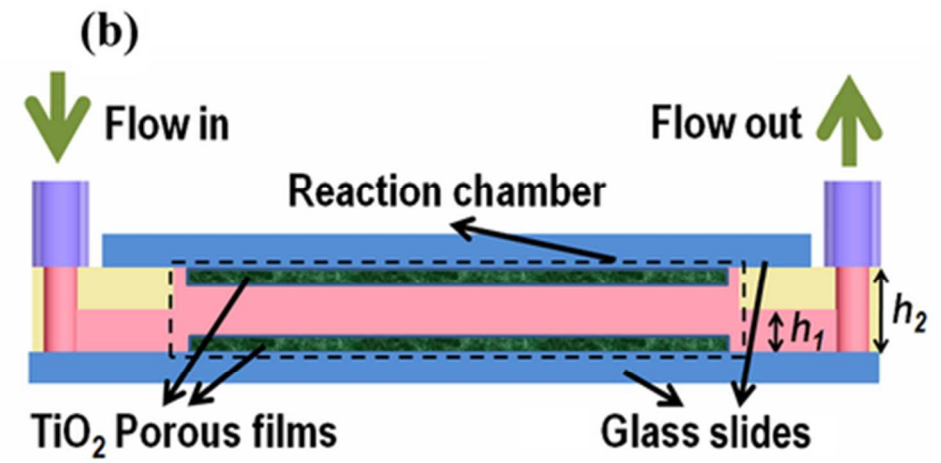

39x19mm (300 x 300 DPI)

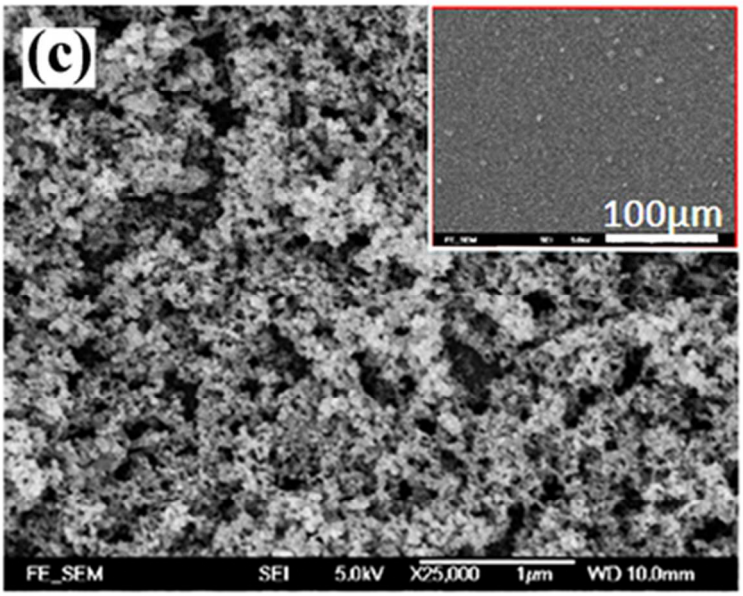

42x26mm (300 x 300 DPI)

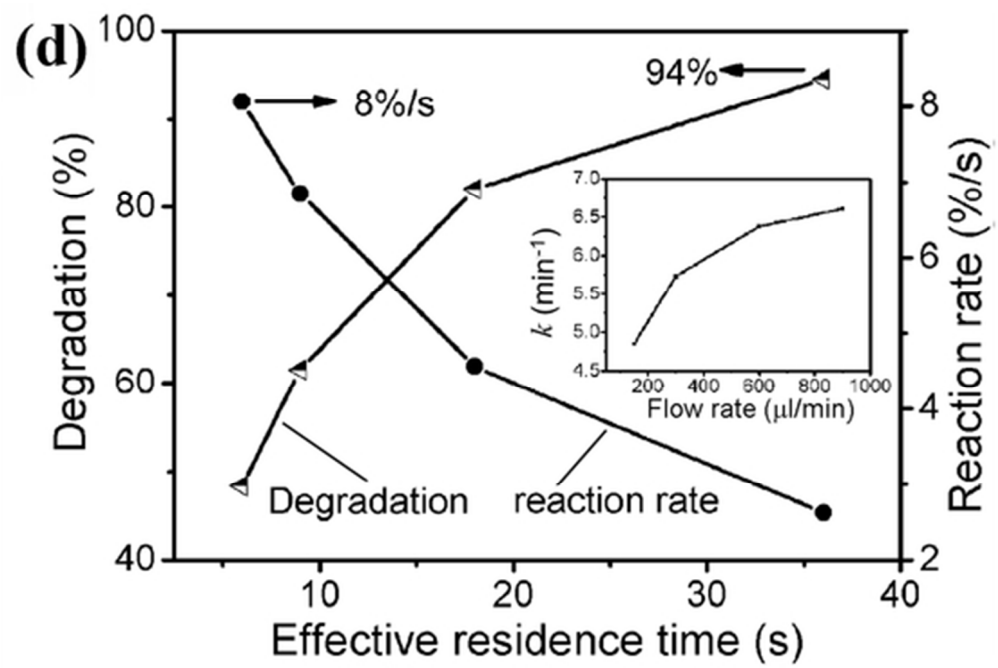

46x31mm (300 x 300 DPI)

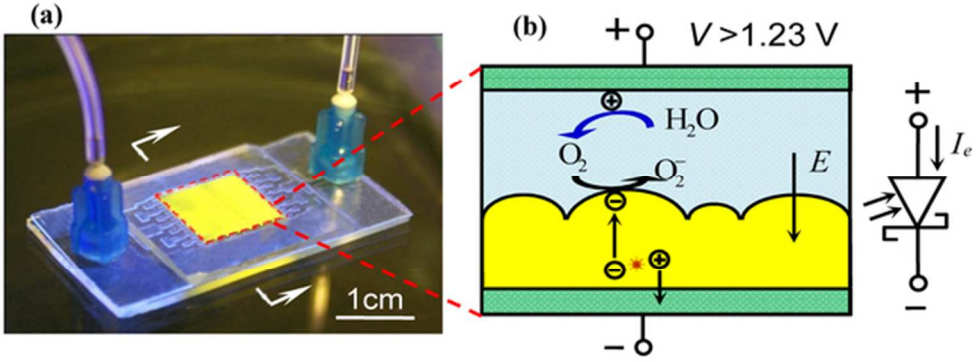

56x21mm (300 x 300 DPI)

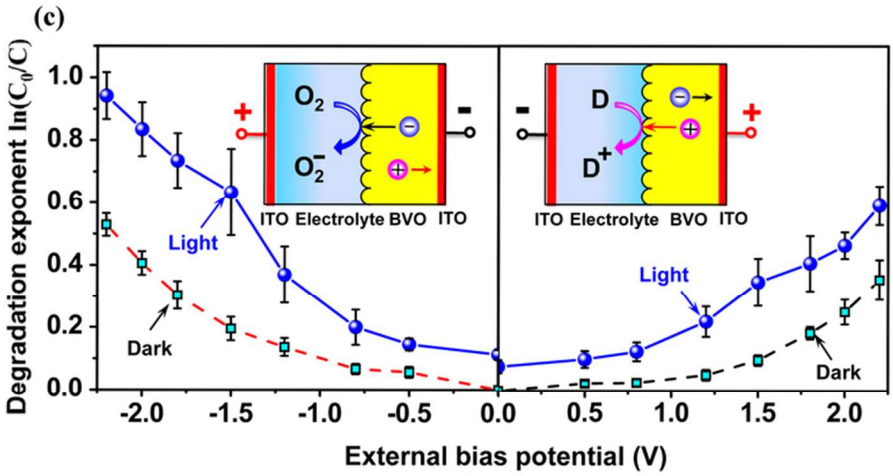

73x35mm (300 x 300 DPI)

Table 1 Typical microfluidic reactors used for photocatalytic water treatment.

Type of microreactor	Catalyst/Light source	Model chemicals
Micro-capillary reactor	TiO_2/SiO_2/UV light	Methylene blue [76]
	TiO_2/UV LED	Rhodamine 6G [77]
	TiO_2/UV lamp	Methylene orange [78]
	TiO_2 /UV LED	Newcoccine, *etc.* [79]
	TiO_2/UV Nd-YAG laser	Salicylic acid [81]
Single straight microchannel reactor	TiO_2/UV led	Chelate（Cu-EDTA）[82]
	P25 TiO_2/UV light	4-chlorophenol [83]
	Pt-TiO_2/UV LED	Methylene blue, *etc.* [71, 80]
Multi-microchannel reactor		
- *Branched microchannel*	TiO_2/UV-A LED	4-chlorophenol [54]
- *Serpentine microchannel*	Nanoporous TiO_2	Methylene blue [48]
	Nanofibrous TiO_2/UV light	Methylene blue [33]
	TiO_2/ Tungsten lamp	Methylene blue/phenol [84]
Planar microreactor	TiO_2/Solar light	Methylene blue [34]
	P25 $TiO_2/BiVO_4$/Solar light	Methylene blue [35]
	$BiVO_4$/Blue LED	Methylene blue [36]